Viscous damping of nanobeam resonators: Humidity, thermal noise, and a paddling effect

Chao Chen,[1,2] Ming Ma,[1,2] Jefferson Zhe Liu,[3] Quanshui Zheng,[1,2] and Zhiping Xu[1,2,a)]
[1]*Department of Engineering Mechanics, Tsinghua University, Beijing 100084, China*
[2]*Center for Nano and Micro Mechanics, Tsinghua University, Beijing 100084, China*
[3]*Department of Mechanical and Aerospace Engineering, Monash University, Clayton, Victoria 3800, Australia*

(Received 26 April 2011; accepted 24 June 2011; published online 15 August 2011)

A nanobeam resonator is a key mechanical component of a nano-electromechanical system. Because of its small dimensions, the system can reach very high frequencies, but it is also very sensitive to its environment, as a large surface area of the material is exposed. Molecular dynamics (MD) simulations and theoretical analysis are used here to quantitatively predict the damping behavior of a nanobeam, including its critical damping conditions and lifetime, directly mapping fluid-structure properties and interaction into dynamics. We show here how the humidity defines the critical damping condition through viscous forces, marking the transition from the under-damping to the over-damping regime at elevated humidity. Phenomena such as thermal fluctuations and the paddling effect are also discussed with an explanation using a simple one-dimensional model. © *2011 American Institute of Physics*. [doi:10.1063/1.3619854]

I. INTRODUCTION

In the past decade there has been rising interest in fabricating mechanical resonators using nanostructures such as carbon nanotubes (CNTs), zinc oxide nanowires, and silicon nanobeams.[1–8] The key advantages of these setups include gigahertz frequencies, more flexible control through electromechanical or opto-mechanical coupling, and the capability to reach the quantum limit of mechanical systems.[9–11] Various applications including sensors, actuators, and relays have been proposed and many of these ideas are already established as building blocks of nanoelectromechanical systems. However, despite the merits already mentioned, practical issues still exist because of perturbations from the surrounding environment, which modify the device behavior significantly at nanoscale.[4] A practical question that is naturally raised is how these devices operate under humid conditions.

In a very recent experiment, carbon nanotube based resonators were used for ultra-sensitive mass sensing in viscous fluids.[4] A resonator was observed to lose its fundamental oscillation once immersed in water, while a number of resonance modes were still distinct in vacuum. This result indicates that, in addition to the intrinsic phononic damping, viscous damping also has an impact on perturbing the vibrational motion of carbon nanotubes. Interesting examples showing the importance of the fluid-structure interaction at a small scale can be widely found in living organisms. Overdamped cytoskeleton fibers provide support and transport functions in the cell. The unique features of the dynamics of these fibers are the dominating contributions from thermal fluctuations, as the bending energy is very low, comparable with the thermal energy k_BT.[12] Thus, thermal fluctuations in a fluid environment provide both viscous damping on the vibration of fibers, as well as driving their motion with noticeable amplitudes.[13–15] The correlation between the thermally induced vibrations and the temperature of the environment is used to estimate the bending rigidity of fibers.[13,16] Moreover, fluid flow can lead to remarkable deformation or motion of slender fibers, which suggests mechanic sensing mechanisms. Some living organisms, *Cupiennius salei* for example, have ultra-vibration-sensitive hairy systems (sensilla) on their body, to detect environmental air flow.[9] In-depth understanding of these systems and phenomena toward bio-inspired applications requires a fundamental investigation on the damping behavior of nanobeam resonators.[17]

In this paper, we investigate the damping behavior of a CNT resonator in a water environment with various humidities. Molecular dynamics (MD) simulations are performed to capture the atomistic mechanism, followed by continuum analysis using the Euler-Bernoulli beam theory. The critical damping condition is defined as a function of the properties of the resonator and the fluid, and also their interactions, which is eventually extended to other representative nanobeam resonators.

II. MODELS AND METHODS

In our MD simulations, we use the LAMMPS package.[18] A single-walled CNT of length, $L_{CNT} = 5.5$ nm, is immersed in a periodic box filled with water. The dimensions of the box are $L_x = 5$ nm and $L_y = 5$ nm in the transverse directions and $L_z = 10$ nm in the direction parallel to the CNT. The extended simple point charge model (SPC/E) model is used for the intra-molecular interactions (bond stretch and bond angle bending) in the water molecules.[19] This model gives a dynamic viscosity $\mu = 0.729$ mPa s, in close agreement with the experimentally measured value 0.896 mPa s.[20] The viscosity is calculated using the Green-Kubo formula in thermal equilibrium, where the viscosity is related to the

a)Author to whom correspondence should be addressed. Electronic mail: xuzp@tsinghua.edu.cn.

autocorrelation function of the off-diagonal components of the stress tensor. MD simulations in the canonical ensemble are performed using the Nosé-Hoover thermostat for 20 to 60 ns to obtain a converged value.[21] The SHAKE algorithm is used to constrain the energy terms involving hydrogen atoms, and to enable a relatively large time step $\Delta t = 0.5$ fs in the simulations.[18] We use the Dreiding force field to model the sp^2 bonding in the CNT, which has been applied in previous models of various carbon nanostructures.[22,23] Van der Waals interactions between the carbon atoms in the CNT and oxygen atoms in the water molecules are described using the Lennard-Jones formula $E_{LJ} = 4\varepsilon[(\sigma/r)^{12} - (\sigma/r)^6]$. This potential function is parameterized to produce the contact angle $\theta_{CA} = 95.3°$ for a water droplet on a graphene sheet, i.e., $\varepsilon = 4.0626$ meV and $\sigma = 0.319$ nm.[24,25]

In our MD simulation, the whole system is first equilibrated at ambient conditions (temperature $T = 300$ K, and pressure $P = 1$ atm) for 100 ps, with a displacement $d = 1$ nm applied to one end of the CNT to initialize the vibration, while the other end of the carbon nanotube is fixed during the simulation.

When immersed in flowing fluid, the carbon nanotube is deflected by the viscous damping force. We calculate the relation between the uniform load F applied transversely on the CNT cantilever beam and its tip deflection d. As shown in Fig. 1, the tip displacement keeps a linear relation with F when d is below 1 nm. Beyond 1 nm, nonlinear effects show up, and eventually radial buckling occurs when d reaches 2 nm.[26] For this reason d is limited to be lower than 1 nm in our simulations, making the linear Euler-Bernoulli beam theory become valid. On the other hand, d is also ensured to be larger than the thermal noise to observe the elasticity-driven mechanisms, whose amplitude is about $0.15 \sim 0.2$ nm, as illustrated by the results summarized in Fig. 2.

At time $t = 0$, the load holding the deflected tip of the carbon nanotube is released, and the CNT starts to retract back due to the elastic restoring force and continues to oscillate if it is not over-damped. Figure 2 shows the tip displacement of the CNT resonator at different nominal humidities H_N, where

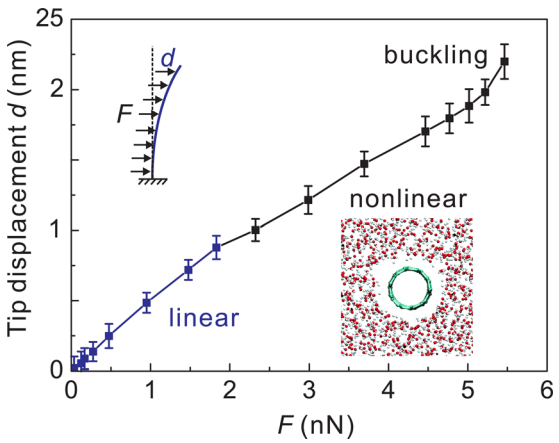

FIG. 1. (Color online) The force-displacement relation for a (10, 10) CNT with a length $L_{CNT} = 5.5$ nm. The load is distributed uniformly along the CNT and deformation is presented by tip displacement d. The behavior can be separated into three regimes, linear elastic ($d < 1$ nm), nonlinear (1 nm $< d < 2$ nm), and post-buckling regime ($d > 2$ nm). Inset: atomic structures of the carbon nanotube and water molecules around it.

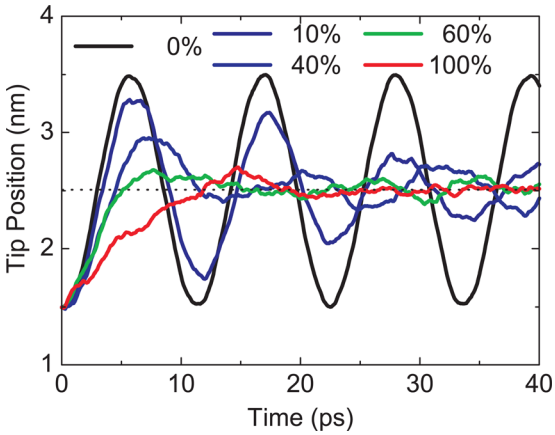

FIG. 2. (Color online) The vibrational evolutions of CNT tip positions at different nominal humidity H_N from 0 to 100%. The difference between under-damping in the vacuum ($H_N = 0$) and over-damping at higher nominal humidities than 40% is clearly shown.

the tip displacement is given by the amplitude of the first-order vibrational mode of the beam. In this work, H_N is defined as the ratio between the density of the water molecules and the equilibrium value of bulk water at 300 K and 1 atm. The conventional definition of humidity is to quantify the amount of water vapor that exists in the air-water vapor mixed environment, which can be investigated using MD methods.[27,28] In this paper, H_N is used as an intuitive representation of the population of water molecules around the solid structure. Other constituents of air such as oxygen and nitrogen molecules are neglected and only the water in a vapor phase is considered. The atomic structures of water molecules around the carbon nanotube at $H_N = 1$ are plotted in Fig. 1, showing a spatially distributed profile without strong clustering at the interface. However as the density of water, or pressure, is lowered, the density profile of water becomes inhomogeneous. The damping force on the resonator therefore depends on the local density, which varies with time. The results discussed in the following sections were obtained as averages of a set of simulations using the same H_N.

III. RESULTS AND DISCUSSION

A. Viscous damping

A series of simulations were performed with H_N ranging from 0 to 100%. Figure 2 shows that the vibrations of the CNT beams are significantly damped in humid environments. In vacuum ($H_N = 0$), a distinct under-damping first-order vibration mode of the CNT is observed, with an ultrahigh frequency $f_1 = 88.9$ GHz originating from the high Young's modulus Y and small aspect ratio. As H_N increases, a significant decay of vibrational amplitude is observed, but the overall behavior in the first several periods is still distinct in the under-damped regime. The phase-shift of the vibration in comparison with the vibration in vacuum is negligible. With an H_N value of 40%, the third peak cannot be distinguished from the noisy background, and the dynamics makes the transition from the under-damping to the over-damping regime. The second peak is still distinct here, but is attributed to the paddling effect, as will be discussed later. Considering

all these results and effects we define the critical damping condition as the H_N value, where the third peak of the tip displacement curve is readable from background noise. By this definition the transition from under-damping to over-damping starts at $H_N \sim 40\%$. Additionally, for all the simulations at $H_N < 40\%$, we notice that the moving tip has a speed $v = 400$ m/s during the first retraction period, indicating an elasticity-driven mechanism. This speed is defined by the bending rigidity of CNTs. However as H_N increases, v decreases to 100 m/s at $H_N = 100\%$, turning into a scenario that features diffusive behavior.

B. The paddling effect

In the previous paragraph, the damping behavior of CNT beam resonators was discussed. It is important to emphasize that the second peak of vibrational amplitude is observed in all the MD simulations without any dependence on humidity or viscosity. It was observed in the MD simulations that after the displaced CNT tip returned to the original position x_0 for the first time, given by the arrow in Fig. 2, it always moved further beyond x_0, even in an over-damping regime, such as for $H_N = 100\%$. This observation contradicts the simple damped oscillator model. In the MD simulations, as the CNT was moving in the water, it caused the surrounding fluid to flow in the same direction. When the CNT tip returned to its original position x_0 and released all the elastic potential energy in bending, it did not stop completely. Instead, small amounts of momentum were transferred back from the surrounding water molecules to the CNT, driving the continuous motion. We call this effect the paddling effect. After the nanobeam lost its elastically driven motion, the tip continued to move due to thermal fluctuations with amplitude of a few angstroms.

To obtain deeper insight into the paddling effect, a modified one-dimension model is provided by including the fluid-structure interaction. In this model, as illustrated in the inset of Fig. 3, a slider at the position x and with a mass m_1 is immersed in a viscous fluid. The slider is also connected to a fixed position in space by a spring with stiffness k, representing the cantilever beam resonator that is studied in the MD simulations. In this nanoscale flow problem with a low Reynolds number, the viscous drag force can be described accurately by the linear creeping flow equation.[29] Denoting the speed of the fluid flow as v, the equilibrium equations for both the slider and fluid can be written as:

$$m_1 d^2x/dt^2 + c(dx/dt - v) + kx = 0 \quad (1a)$$

$$m_2 dv/dt - c(dx/dt - v) = 0 \quad (1b)$$

where m_2 is the mass of the fluid, and c is the drag coefficient. For a cylindrical structure like a carbon nanotube that is immersed in viscous flow the drag coefficient is $c = C\mu L_{CNT}/2$, where C_d is the viscous damping coefficient and $C = C_d \mathrm{Re}$. We then have

$$d^2x/dt^2 + 2\xi\omega_0(dx/dt - v) + \omega_0^2 x = 0 \quad (2a)$$

$$m * dv/dt - 2\xi\omega_0(dx/dt - v) = 0 \quad (2b)$$

where $m^* = m_2/m_1$, $\omega_0 = (k/m_1)^{1/2}$ and $\xi = c/2m_1\omega_0$.

The initial displacement amplitude d can be used as a reference for the length scale and $1/\omega_0 = (m_1/k)$[1] as a reference for the time scale, giving the equations a dimensionless form

$$d^2\underline{x}/d\underline{t}^2 + 2\xi(d\underline{x}/d\underline{t} - \underline{v}) + \underline{x} = 0 \quad (2c)$$

$$m * d\underline{v}/d\underline{t} - 2\xi(d\underline{x}/d\underline{t} - \underline{v}) = 0 \quad (2d)$$

Here $\underline{x} = x/d$, $\underline{t} = t\omega_0$, and $\underline{v} = v/d\omega_0$.

As it is difficult to find analytical solutions for Eqs. (2c) and (2d), numerical solutions are obtained using finite difference methods. Figure 3 shows the curve of damped vibrational amplitude with initial conditions $x(0) = -1$ and $v(0) = 0$. m^* is set to be 15, accordingly. In this case, the paddling effect influences the damping behavior when it reaches the critical value $\xi = 1$, where the slider always moves back over the equilibrium position $x = 0$. Moreover, in a clearly over-damped regime the paddle effect still exists ($\xi = 1.5$), which is consistent with MD simulations.

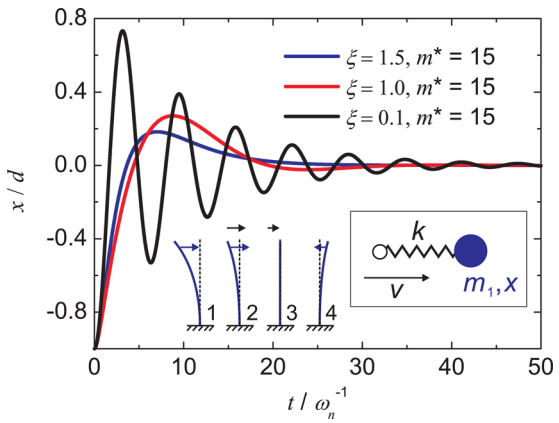

FIG. 3. (Color online) The damped vibrational amplitudes of the nanobeam resonators where the paddling effect is included, obtained as solutions of the one-dimensional model (Eqs. (2c) and 2(d)). Insets: an illustration of the paddling effect and the analytic model proposed in this work.

C. A viscous damping model

The MD simulations, although providing atomic details of the whole dissipation process, cannot be extended to the large length scales of the widely spanned fluid medium and structural materials that are encountered in the design of micro and nanoelectromechanical systems. A theoretical analysis based on the Euler-Bernoulli beam theory[14] was performed to overcome this limitation. The mechanical vibration of an elastic beam can be described by the equation

$$D\partial^4 w/\partial x^4 + \rho A\partial^2 w/\partial t^2 + C_\mu/2\partial w/\partial t = 0 \quad (3)$$

where w is the deflection of the CNT, t represents time, and x is the position along the carbon nanotube. Y is the Young' s modulus, I is the bending moment of inertia of the CNT, and $D = YI$ is the bending rigidity. ρ is the mass density and A is the cross-sectional area. C is the drag coefficient and μ is the dynamic viscosity of the fluid.

To determine C, MD simulations are performed for water flow around a CNT with the same geometry. For flow in and around nanostructures, the Reynolds number is

usually very low, as $\mathrm{Re} = \rho u l/\mu < 0.4$, where ρ is the density of water at the ambient condition, and l is the characteristic length scale of the structure. Here we use $l = D$, the diameter of the CNT, and find that even at a respectable flow rate ($u_{\max} \sim 400$ m/s) $\mathrm{Re} = 0.37$ is still low. From MD simulations where water flow is induced around carbon nanotubes, we find that at low $\mathrm{Re} < 0.3$, the Stokes law $C_d = C/\mathrm{Re}$ works well in fitting the simulation results and it yields $C = 4.467$.

For the cantilever beam, one end of the beam ($x = 0$) is fixed and the other end ($x = L_{\mathrm{CNT}}$) is free. By substituting these boundary conditions, i.e., $w(0, t) = \partial w/\partial x(0, t) = \partial^2 w/\partial x^2(L_{\mathrm{CNT}}, t) = \partial^3 w/\partial x^3(L_{\mathrm{CNT}}, t) = 0$ into Eq. (3), we obtain the eigenfrequencies for vibrational modes n in the absence of damping by

$$\omega_n = \beta_n^2/L^2\sqrt{D/\rho A}. \quad (4)$$

where β is a numerical factor specific for each vibrational mode. For mode i ($= 1, 2, \ldots$), $\beta_i = 1.875, 4.694, \ldots$.[30]

In the under-damping regime, the solution of Eq. (3) is still oscillating but the vibrational frequency is shifted.[16] The amplitude $A(t)$ of vibration decays exponentially, i.e., $A(t) = A(0)\exp(-\xi\omega t)$ and the frequency is:

$$\omega_n' = \omega_n\sqrt{1-\xi^2}, 0 < \xi = C\mu L^2/\left(4\beta_n^2\sqrt{\rho AD}\right) < 1. \quad (5)$$

Close inspection of the results in Fig. 2 indicates that the amplitude A exhibits an exponential decay, which can be used to obtain a fit for the damping coefficient, ξ. The quality factor Q, which is used to quantify the damping effects in the under-damped regime, can be calculated as $Q = 1/(2\xi)$. The results are shown in Fig. 4. As the humidity increases, the quality factor is reduced from the order of 10^3 in vacuum to 28 at $H_{\mathrm{N}} = 2\%$, and further reduced to under 5 when H_{N} exceeds 12%. As a result of the paddling effect it is difficult to define a reasonable Q value as it is close to 0.5 ($\xi = 1$), under critical damping conditions.

In the over-damped regime, the oscillation behavior of the beam-resonators is heavily inhibited and one full period of vibration cannot be completed. The frequency becomes

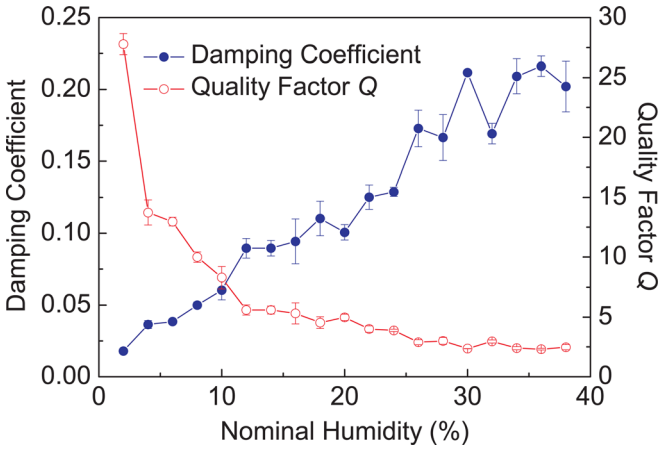

FIG. 4. (Color online) Damping coefficients ξ and quality factors Q as obtained from molecular dynamics simulations at different nominal humidities H_{N} from 0 to 40%.

$$\omega_n' = \omega_n\sqrt{\xi^2 - 1}, \xi > 1. \quad (6)$$

Figure 2 shows such over-damped vibration at nominal humidities of 60% and 100%.

D. Lifetime of the resonator

The function of a CNT resonator with over-damped vibrations actually turns into a relay, and the key variable to quantify its dynamical behavior is not the quality factor Q, but the lifetime of the initialized vibration, or the *returning time* to the equilibrium position x_0. For the humidity $H_{\mathrm{N}} > 10\%$, the vibration energy dissipates within a relatively short time scale of tens of picoseconds. For under-damped vibrations, the oscillation amplitude decays exponentially as $A = A_0\exp(-\xi\omega_{\mathrm{n}}t)$. Here the lifetime is defined as $\tau = (\xi\omega_{\mathrm{n}})^{-1} = 4\rho A/C\mu$, which implies that the vibrational amplitude decays to 36.8% within the time range τ. For most of the ξ values in Fig. 4 with $H_{\mathrm{N}} > 10\%$, ξ is larger than 0.05. So the lifetime is estimated to be shorter than 35.8 ps. Although the total simulation time is longer, Fig. 2 only shows the damping curves for the first 40 picoseconds, because this captures the whole damping process in most of the cases.

E. Critical damping

Identifying the transition from under-damping to over-damping is crucial to designing micro- and nano-resonators. Because of the influences of thermal noise and the paddling effect, it is difficult to strictly identify this transition directly from MD simulations. From the Euler-Bernoulli beam theory, by comparing equations (5) and (6) and by neglecting the thermal fluctuations and the paddling effect as observed in MD simulations, the critical damping can be defined by $\xi = 1$, i.e.,

$$\mu_{c,n} = 4\beta_n^2\sqrt{\rho AD}/CL^2 \quad (7)$$

and for the first-order vibrational mode it is $\mu_{c,1} = 14\sqrt{\rho AD}/CL^2$.

From Eq. (7) we can see that not only the structural properties (D, A, ρ, and L) of the beam, but also the fluid (μ_c) and the fluid-structure interaction parameters (C) play a role in defining the critical damping. For a number of types of nanobeams, the behavior of their vibration motion in various fluid environments is predicted, as summarized in Fig. 5. For the single-walled CNT (diameter $d = 1.4$ nm as we investigated using MD simulations), a fluidic viscosity leads to over-damping for length L larger than 5 nm. However, in air it works by an under-damping mechanism. It should be mentioned here that for air molecules, as the mean free path can be comparable to or larger than the dimension of nanofibers, free molecule flow theory needs to be used to predict precisely the damping force in Eq. (3). The silicon carbide ($d = 20$ nm, $L = 1$ μm) and zinc oxide beam resonators ($d = 50$ nm, $L = 1$ μm) are over-damped and under-damped, respectively. For a microtubule ($d = 50$ nm, $L = 5$ μm), the bending motion is heavily over-damped due to the relatively low bending rigidity and large aspect ratio. The conclusion from these results can be used to design nano-electromechanical systems in an

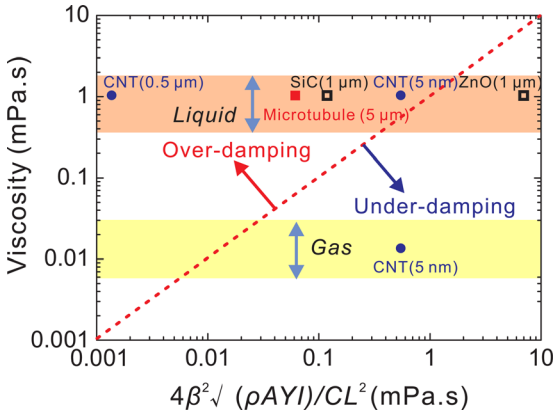

FIG. 5. (Color online) Damping behaviors of different types of nano- and micro-fibers, as immersed in various environmental fluids from water to air. The diameters of carbon nanotubes, silicon carbide, zinc oxide beams, and microtubules are considered to be 1.4, 20, 50, and 50 nm respectively. The lengths are depicted in parentheses.

aqueous or gaseous environment, enabling devices from resonators in under-damped conditions to relays in over-damped conditions. Also they could help to improve the understanding of biomechanical systems related to fluid environments, such as cytoskeleton networks and the hairy mechanosensing and energy harvesting systems of some insects.

IV. CONCLUSION

In summary, the viscous damping on nanobeam resonators was investigated. The effects of humidity, viscosity, and phenomena including thermal noise and the paddling effect were discussed based on results from MD simulations and theoretical analysis. Analytical models were proposed and used to obtain the critical damping conditions and lifetime of nanobeam resonators. The results obtained here provide detailed information about nanoscale fluid-structure interactions and can be applied both in designing nanoelectromechanical systems and in understanding related biomechanical systems.

ACKNOWLEDGMENTS

This work is supported by Tsinghua University through the Key Talent Support Program, and the National Science Foundation of China through Young Scholar Grants 11002079, No. 10872114, No. 10672089, and No. 10832005. This work is also supported by the Shanghai Supercomputer Center of China.

[1]V. Sazonova, Y. Yaish, H. Ustunel, D. Roundy, T. A. Arias, and P. L. McEuen, Nature **431**(7006), 284 (2004).
[2]S. S. Verbridge, R. Ilic, H. G. Craighead, and J. M. Parpia, Appl. Phys. Lett. **93**(1), 013101 (2008).
[3]H. B. Peng, C. W. Chang, S. Aloni, T. D. Yuzvinsky, and A. Zettl, Phys. Rev. Lett. **97**(8), 087203 (2006).
[4]S. Sawano, T. Arie, and S. Akita, Nano Lett. **10**(9), 3395 (2010).
[5]X. M. H. Huang, C. A. Zorman, M. Mehregany, and M. L. Roukes, Nature **421**(6922), 496 (2003).
[6]K. Eom, H. S. Park, D. S. Yoon, and T. Kwon, Phys. Rep. **503**(4–5), 115 (2011).
[7]Q. Quan, P. B. Deotare, and M. Loncar, Appl. Phys. Lett. **96**(20), 203102 (2010).
[8]P. B. Deotare, M. W. McCutcheon, I. W. Frank, M. Khan, and M. LonCar, Appl. Phys. Lett. **94**(12), 121106 (2009).
[9]K. Kim, K. Jensen, and A. Zettl, Nano Lett. **9**(9), 3209 (2009).
[10]H. Jiang, M. F. Yu, B. Liu, and Y. Huang, Phys. Rev. Lett. **93**(18), 185501 (2004).
[11]J. L. Arlett, E. B. Myers, and M. L. Roukes, Nature Nanotechnol. **6**(4), 203 (2011).
[12]D. A. Fletcher and R. D. Mullins, Nature **463**(7280), 485 (2010).
[13]M. M. J. Treacy, A. Krishnan, and P. N. Yianilos, Microsc. Microanal. **6**(4), 317 (2000).
[14]Z. Xu, Q.-S. Zheng, and G. Chen, Phys. Rev. B **75**(19), 195445 (2007).
[15]Z. Xu, R. Paparcone, and M. J. Buehler, Biophys. J. **98**(10), 2053 (2010).
[16]M. M. J. Treacy, T. W. Ebbesen, and J. M. Gibson, Nature **381**(6584), 678 (1996).
[17]C. Liu, Bioinspiration Biomimetics **2**(4), S162 (2007).
[18]S. Plimpton, J. Comput. Phys. **117**(1), 1 (1995).
[19]H. J. C. Berendsen, J. R. Grigera, and T. P. Straatsma, J. Phys. Chem. **91**(24), 6269 (1987).
[20]M. A. Gonzalez and J. L. F. Abascal, J. Chem. Phys. **132**(9), 096101 (2010).
[21]G. Guo and Y. Zhang, Mol. Phys. **99**(4), 283 (2001).
[22]Z. Xu, Q. Zheng, Q. Jiang, C.-C. Ma, Y. Zhao, G. Chen, H. Gao, and G. Ren, Nanotechnology **19**(25), 255705 (2008).
[23]Y. Guo, N. Karasawa, and W. A. Goddard, Nature **351**(6326), 464 (1991).
[24]M. D. Ma, L. Shen, J. Sheridan, J. Z. Liu, C. Chen, and Q. Zheng, Phys. Rev. E **83**(3), 036316 (2011).
[25]D. Mattia and Y. Gogotsi, Microfluid. Nanofluid. **5**(3), 289 (2008).
[26]J. Z. Liu, Q. Zheng, and Q. Jiang, Phys. Rev. Lett. **86**(21), 4843 (2001).
[27]V. V. Chaban and O. V. Prezhdo, ACS Nano **5**(7), 5647 (2011).
[28]R. Srivastava, H. Docherty, J. K. Singh, and P. T. Cummings, J. Phys. Chem. C **115**(25), 12448 (2011).
[29]J. H. Walther, T. Werder, R. L. Jaffe, and P. Koumoutsakos, Phys. Rev. E **69**(6), 062201 (2004).
[30]W. J. Weaver, S. P. Timoshenko, and D. H. Young, *Vibration Problems in Engineering*, 5th ed. (Wiley-Interscience, Hoboken, NJ, 2001).